





ARTICLE

Open Access

# Inhibition of mPGES-1 attenuates efficient resolution of acute inflammation by enhancing CX3CL1 expression

Peter Rappl<sup>1</sup>, Silvia Rösser<sup>1</sup>, Patrick Maul<sup>1</sup>, Rebekka Bauer<sup>1</sup> , Arnaud Huard<sup>1</sup>, Yannick Schreiber<sup>2</sup>, Dominique Thomas<sup>3</sup>, Gerd Geisslinger<sup>2,3</sup>, Per-Johan Jakobsson<sup>4</sup>, Andreas Weigert<sup>1</sup> , Bernhard Brüne<sup>1,2,5,6</sup>  and Tobias Schmid<sup>1</sup> 

## Abstract

Despite the progress to understand inflammatory reactions, mechanisms causing their resolution remain poorly understood. Prostanoids, especially prostaglandin E<sub>2</sub> (PGE<sub>2</sub>), are well-characterized mediators of inflammation. PGE<sub>2</sub> is produced in an inducible manner in macrophages (M $\phi$ ) by microsomal PGE<sub>2</sub>-synthase-1 (mPGES-1), with the notion that it also conveys pro-resolving properties. We aimed to characterize the role of mPGES-1 during resolution of acute, zymosan-induced peritonitis. Experimentally, we applied the mPGES-1 inhibitor compound III (CIII) once the inflammatory response was established and confirmed its potent PGE<sub>2</sub>-blocking efficacy. mPGES-1 inhibition resulted in an incomplete removal of neutrophils and a concomitant increase in monocytes and M $\phi$  during the resolution process. The mRNA-seq analysis identified enhanced C-X<sub>3</sub>-C motif receptor 1 (CX3CR1) expression in resident and infiltrating M $\phi$  upon mPGES-1 inhibition. Besides elevated *Cx3cr1* expression, its ligand CX3CL1 was enriched in the peritoneal lavage of the mice, produced by epithelial cells upon mPGES-1 inhibition. CX3CL1 not only increased adhesion and survival of M $\phi$  but its neutralization also completely reversed elevated inflammatory cell numbers, thereby normalizing the cellular, peritoneal composition during resolution. Our data suggest that mPGES-1-derived PGE<sub>2</sub> contributes to the resolution of inflammation by preventing CX3CL1-mediated retention of activated myeloid cells at sites of injury.

## Introduction

Inflammatory responses are essential for an effective host defense against pathogenic threats such as invading bacteria or viruses<sup>1,2</sup>. The onset of acute inflammation is typically characterized by a rapid and fulminant influx of neutrophils, i.e. polymorphonuclear cells (PMN), into inflamed tissues, where they form a first line of defense to eliminate pathogens. Thereafter, monocytes (MO) are

recruited, followed by their differentiation into distinct macrophage (M $\phi$ ) subsets. M $\phi$  not only phagocytose invading pathogens and present them via their major histocompatibility complexes (MHC) to the adaptive immune system, they also remove short-lived, dying neutrophils in a process known as efferocytosis<sup>3–5</sup>. The uptake of apoptotic cells alters the phenotype of M $\phi$  from a pro-inflammatory to an immune-regulatory one<sup>6–9</sup>, thereby contributing to the resolution of inflammation, i.e. normalization of tissue homeostasis<sup>10–12</sup>. Effective resolution of inflammation is important to avoid tissue damage by producing uncontrolled destructive signals. Unfortunately, the transition from inflammation to its resolution remains incompletely understood. There is increasing evidence that the resolution phase is already initiated early during onset of inflammation and that

Correspondence: Bernhard Brüne ([b.bruene@biochem.uni-frankfurt.de](mailto:b.bruene@biochem.uni-frankfurt.de)) or Tobias Schmid ([t.schmid@biochem.uni-frankfurt.de](mailto:t.schmid@biochem.uni-frankfurt.de))

<sup>1</sup>Institute of Biochemistry I, Faculty of Medicine, Goethe-University Frankfurt, Frankfurt, Germany

<sup>2</sup>Fraunhofer Institute for Translational Medicine and Pharmacology, Frankfurt, Germany

Full list of author information is available at the end of the article  
These authors contributed equally: Bernhard Brüne, Tobias Schmid.  
Edited by B. Zhivotovsky

© The Author(s) 2021



**Open Access** This article is licensed under a Creative Commons Attribution 4.0 International License, which permits use, sharing, adaptation, distribution and reproduction in any medium or format, as long as you give appropriate credit to the original author(s) and the source, provide a link to the Creative Commons license, and indicate if changes were made. The images or other third party material in this article are included in the article's Creative Commons license, unless indicated otherwise in a credit line to the material. If material is not included in the article's Creative Commons license and your intended use is not permitted by statutory regulation or exceeds the permitted use, you will need to obtain permission directly from the copyright holder. To view a copy of this license, visit <http://creativecommons.org/licenses/by/4.0/>.

interfering with early inflammatory reactions alters resolution as well<sup>11,13</sup>. Along these lines, recent studies indicated that the well-established pro-inflammatory lipid mediator prostaglandin E<sub>2</sub> (PGE<sub>2</sub>)<sup>14</sup> also bears pro-resolving properties<sup>15–20</sup>. This is of interest, since non-steroidal anti-inflammatory drugs (NSAIDs), which are the main class of non-prescribed, over the counter anti-inflammatory drugs, target cyclooxygenases to inhibit the production of prostanoids, most notably PGE<sub>2</sub><sup>21,22</sup>. More specific inhibitors of PGE<sub>2</sub> production have recently been developed to target the terminal synthase active under inflammatory conditions, i.e. the microsomal PGE<sub>2</sub> synthase-1 (mPGES-1)<sup>23–25</sup>.

In this study, we explored the role of PGE<sub>2</sub> during resolution of inflammation. Experimentally, we blocked PGE<sub>2</sub> production in a zymosan-induced peritonitis model, selectively during the resolution phase using a specific mPGES-1 inhibitor<sup>26</sup>.

## Results

### Inhibition of mPGES-1 alters resolution of zymosan-induced peritonitis

While the role of prostanoids, especially PGE<sub>2</sub>, during the initial phase of inflammation is well characterized, its impact towards resolution of inflammation remains largely elusive. To better understand how PGE<sub>2</sub> contributes to late inflammatory processes, we induced a self-limiting peritonitis in C57/BL6 mice by intraperitoneal (i.p.) injection of zymosan (5 mg/kg), and inhibited PGE<sub>2</sub> synthesis by daily i.p. injections of the selective mPGES-1 inhibitor CIII (25 mg/kg)<sup>26</sup> once the inflammatory response was established for 24 h (Fig. 1A). FACS analyses (gating strategy see Supplementary Fig. 1) supported the transient character of the peritonitis model as the massive increase of leukocytes (CD45<sup>+</sup>) observed at day 1 was reversed starting at day 3. Inhibition of mPGES-1 attenuated this decrease, resulting in higher leukocyte numbers in the peritoneum at days 3 and 6 (Fig. 1B). With respect to neutrophils (PMN), the major cellular infiltrates during inflammation, we noticed only a small increase in cell numbers comparing vehicle control (VEH)- vs. CIII-treated mice at day 6 (Fig. 1C). Since Mφ coordinate early as well as late inflammatory processes, we next determined the presence of MO and Mφ. There was a massive infiltration of MO at day 1, which returned to basal levels at day 6 in VEH-treated mice. In contrast, MO numbers started to increase again at day 6 compared to day 3 upon mPGES-1 inhibition (Fig. 1D). Importantly, two subsets of Mφ are found in the peritoneum, F4/80<sup>lo</sup>, MerTK<sup>lo</sup> Mφ, which are considered as infiltrating Mφ of monocytic origin, and F4/80<sup>hi</sup>, MerTK<sup>hi</sup> Mφ, which represent the resident Mφ population, either of mesodermal descent or differentiated from infiltrating Mφ<sup>27,28</sup>. In control animals, F4/80<sup>lo</sup> Mφ number behaved similarly

to MO although their increase was less pronounced at day 1, returning to baseline levels at day 6 (Fig. 1E). CIII-treatment showed higher numbers of F4/80<sup>lo</sup> Mφ at day 3, which further increased at day 6 compared to controls. In contrast, the number of F4/80<sup>hi</sup> Mφ steadily decreased over time in control animals but remained at high, starting levels, when mPGES-1 was blocked (Fig. 1F). Determination of PGE<sub>2</sub> concentrations in the peritoneal lavage validated the efficacy of CIII to prevent an increase of PGE<sub>2</sub> especially at early times of resolution, i.e. at day 3 (Fig. 1G). It appears that PGE<sub>2</sub> is needed to normalize the myeloid cell composition during resolution of inflammation in zymosan-induced, acute peritonitis.

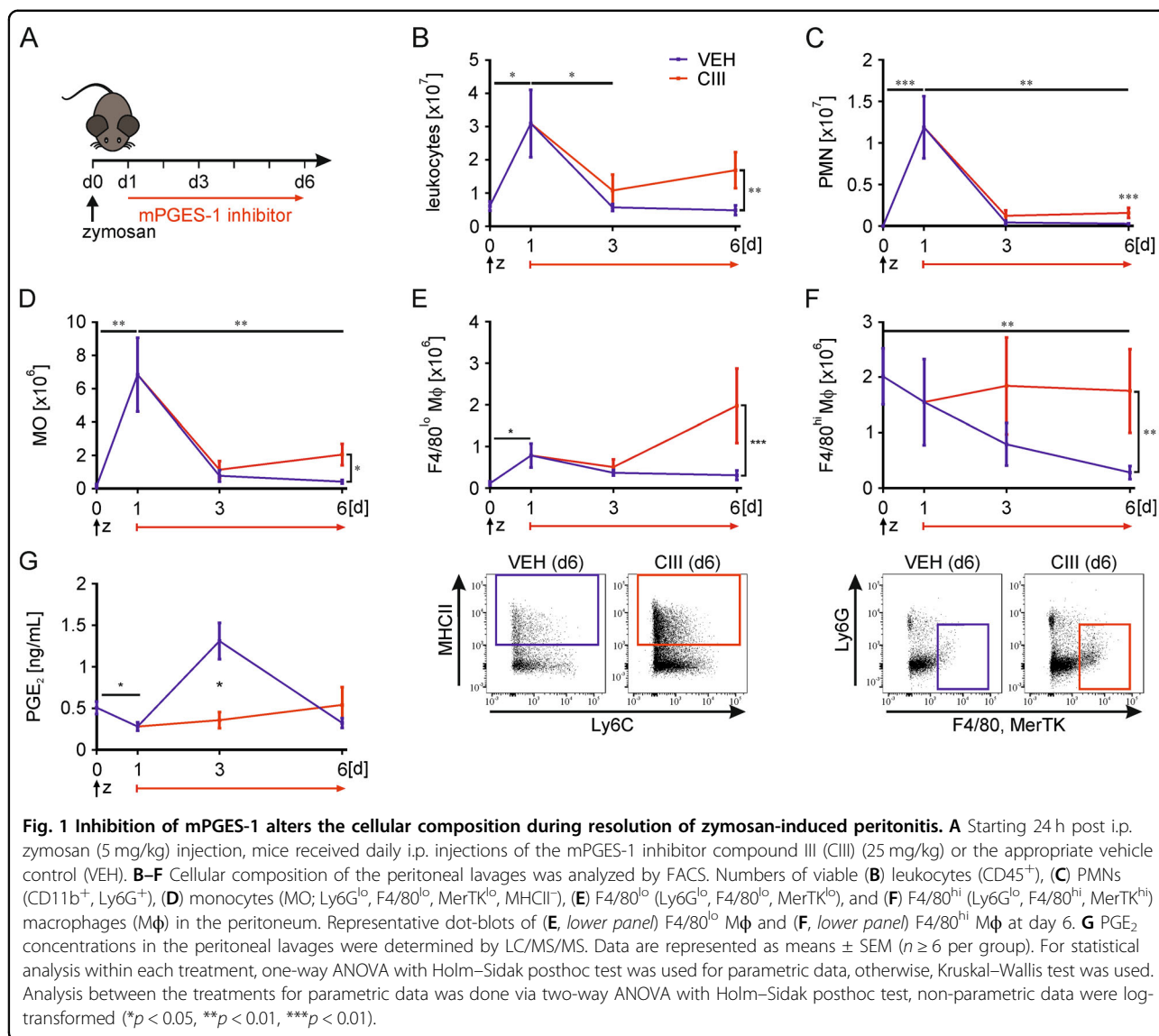
### Inhibition of mPGES-1 alters the macrophage resolution phenotype

As PGE<sub>2</sub> affects the number of Mφ during resolution of inflammation, we were interested to explore whether their polarization is affected as well. To this end, we determined transcriptome changes in F4/80<sup>lo</sup> and F4/80<sup>hi</sup> Mφ subpopulations (Fig. 1E, F) by mRNA-sequencing. Amongst the top 250 differentially expressed genes (DEGs) in F4/80<sup>lo</sup> Mφ (Fig. 2A, Supplementary Table 1) 95 genes were upregulated when mPGES-1 was blocked. These showed an enrichment in GO terms towards immune cell activation processes (Fig. 2B), while the downregulated genes revealed GO terms associated with chemotaxis and migration (Fig. 2C). In F4/80<sup>hi</sup> Mφ, the 60 upregulated candidates amongst the top 250 DEGs (Fig. 2D, Supplementary Table 2) showed a pronounced enrichment in processes linked to antigen processing and presentation via MHCII (Fig. 2E), while GO terms linked to metabolic processes were found in the downregulated targets (Fig. 2F). Interestingly, only 19 of the top 250 DEGs were shared between F4/80<sup>lo</sup> and F4/80<sup>hi</sup> Mφ (Fig. 2G). Of these, six were upregulated (including CX3C motif chemokine receptor 1 (Cx3cr1), integrin β7 (Itgb7), and H2-Eb1), while 13 were downregulated upon mPGES-1 inhibition (including C–C motif chemokine ligand 12 (Ccl12) and fatty acid-binding protein 5 (Fabp5)).

These data imply that inhibition of mPGES-1 activity during resolution of inflammation not only affects inflammatory cell numbers but also their activation profile.

### Inhibition of mPGES-1 enhances the CX3CL1-CX3CR1 axis

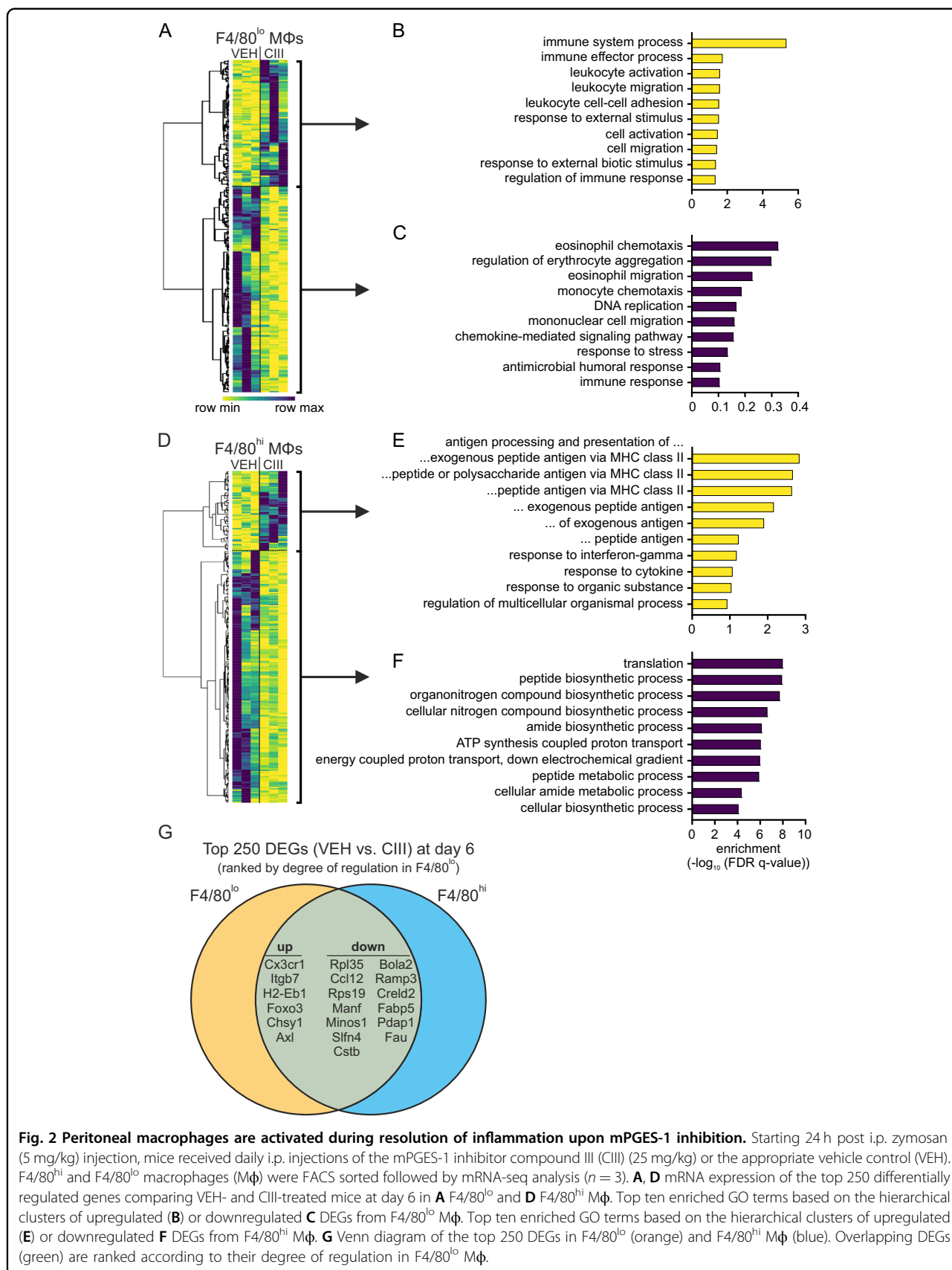
Knowing that inhibition of mPGES-1 increases Mφ numbers during resolution of inflammation, we next asked if the enhanced expression of the well-established myeloid chemokine receptor CX3CR1 might provide a mechanistic explanation. Validation of *Cx3cr1* mRNA kinetics supported a significant increase at day 6 upon CIII-treatment in FACS-sorted F4/80<sup>lo</sup> (Fig. 3A) and F4/

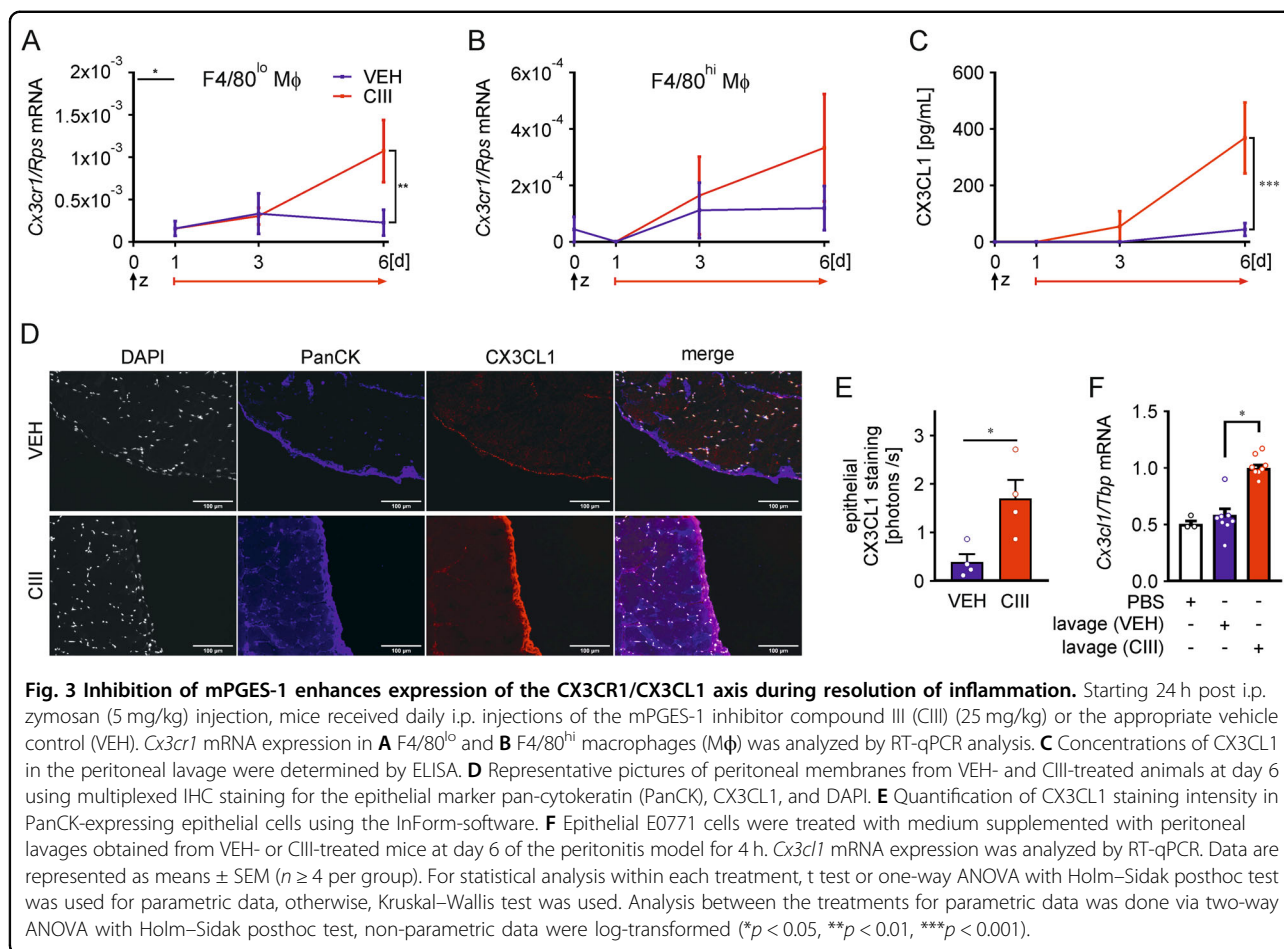


80<sup>hi</sup> Mφ (Fig. 3B), although less pronounced in the latter ones. Considering that there is only one known ligand for CX3CR1, namely CX3C motif chemokine ligand 1 (CX3CL1, also known as fractalkine)<sup>29,30</sup>, we determined the concentration of this chemokine in peritoneal lavages. CX3CL1 was absent in naive mice or 1 day after zymosan injection, remained low in VEH-treated animals, but continuously increased in mice that received CIII (Fig. 3C). Thus, limiting mPGES-1-derived PGE<sub>2</sub> might attenuate the recruitment of Mφ by interfering with the production of CX3CL1.

Since *Cx3cl1* mRNA was not detectable in any of the Mφ subpopulations tested in our model, but has been shown as a product of epithelial and endothelial cells<sup>31</sup>, we isolated peritoneal membranes from mice at day 6 following zymosan injection and used multiplexed

immunohistochemistry (IHC) to determine the local source of this chemokine. Co-localization of CX3CL1 with the epithelial marker pan-cytokeratin (PanCK) in both, VEH- and CIII-treated conditions supported epithelial production of CX3CL1 (Fig. 3D). Automated quantification using a trainable segmentation algorithm further revealed that mPGES-1 inhibition significantly increased epithelial CX3CL1 expression as compared to VEH-controls (Fig. 3E). To validate mPGES-1-dependent CX3CL1 regulation, we exposed murine epithelial E0771 cells in vitro to medium supplemented with peritoneal lavages obtained from mice at day 6 of the peritonitis model. Medium supplemented with lavage fluid from CIII-treated animals enhanced *Cx3cl1* mRNA expression in epithelial cells, while supplementation with VEH-control lavages left the chemokine expression



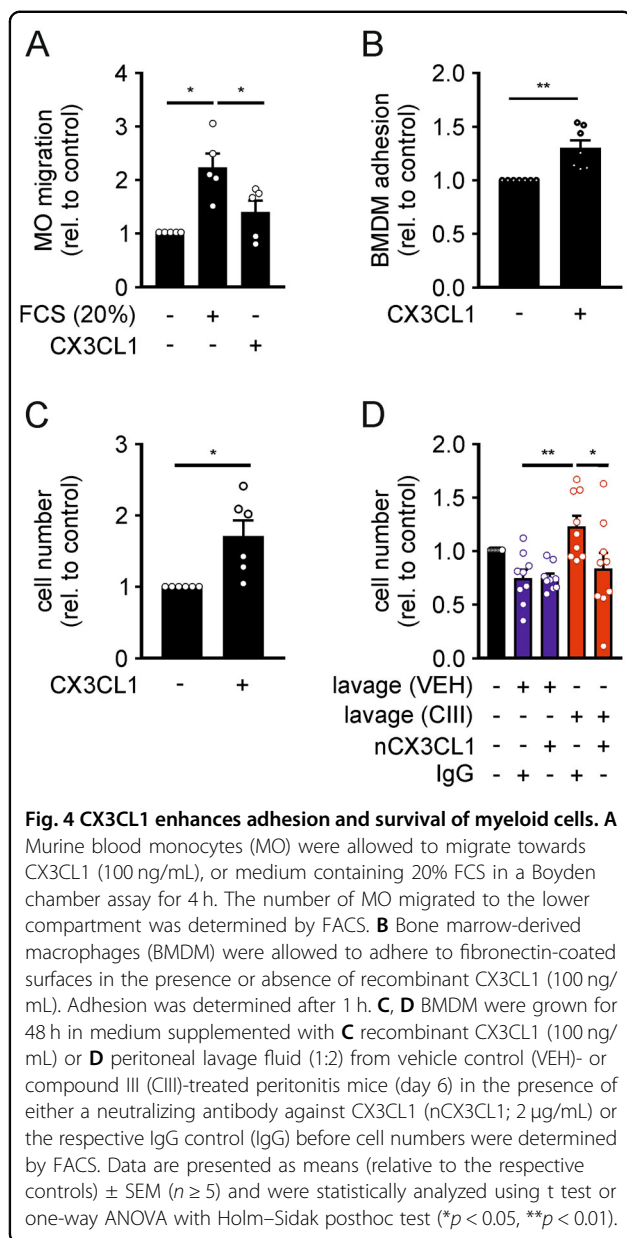


unaltered relative to the controls (Fig. 3F). Inhibition of mPGES-1 apparently enhanced epithelial expression of CX3CL1, which adds to increase Mφ numbers in the peritoneal cavity during resolution of zymosan-induced peritonitis.

### CX3CL1 is critical for Mφ presence in response to mPGES-1 inhibition

CX3CL1 is known for its chemoattractive, pro-adhesive, and pro-survival/proliferating effects on mononuclear phagocytes<sup>32–34</sup>. Therefore, we determined the migration-modulating properties of CX3CL1 by allowing MO to migrate for 4 h in a Boyden chamber transwell assay towards CX3CL1 (100 ng/mL). While MO migrated towards the positive control (20% FCS), they did not migrate towards CX3CL1 (Fig. 4A and Supplementary Fig. 2A). Since *Itgb7* ranged high among the DEGs upregulated at day 6 upon CIII-treatment (Fig. 2G), we addressed changes in Mφ adhesion to fibronectin (FN) in response to CX3CL1. To this end, differentiated bone marrow-derived macrophages (BMDM) were allowed to adhere to FN-coated surfaces. After 1 h we observed significantly more adherent BMDM after stimulation with CX3CL1

(100 ng/mL) compared to controls (Fig. 4B and Supplementary Fig. 2B). To assess if CX3CL1 might also affect Mφ numbers by altering their proliferation or survival, we stained BMDM with carboxyfluorescein succinimidyl ester (CFSE) and determined both cell number as well as the reduction in mean CFSE (as an indicator of proliferation) after 48 h in the presence or absence of CX3CL1 (100 ng/mL). While proliferation was not affected by CX3CL1 (Supplementary Fig. 2C), higher Mφ numbers were observed in response to CX3CL1 (Fig. 4C). Furthermore, supplementing media with day 6 peritoneal lavages of zymosan- and CIII-treated mice, resulted in higher cell numbers compared to supplementation with lavages from VEH-treated animals (Fig. 4D), while the proliferation rates remained unaltered (Supplementary Fig. 2D). To test if CX3CL1 within the peritoneal lavages might be involved, we depleted CX3CL1 using a neutralizing antibody (nCX3CL1, 2 μg/mL). This approach completely abolished increased cell numbers in response to lavages of CIII-treated animals (Fig. 4D). Corroborating previous reports that CX3CL1 enhances survival by inducing expression of anti-apoptotic Bcl2 (ref. <sup>34,35</sup>), *Bcl2* expression was elevated in F4/80<sup>hi</sup> Mφ upon mPGES-1



inhibition (Supplementary Table 2). These observations further support the notion that elevated CX3CL1 levels in response to mPGES-1 inhibition contributed to increase M $\phi$  numbers during late-phase resolution, likely by enhancing their adhesion and survival.

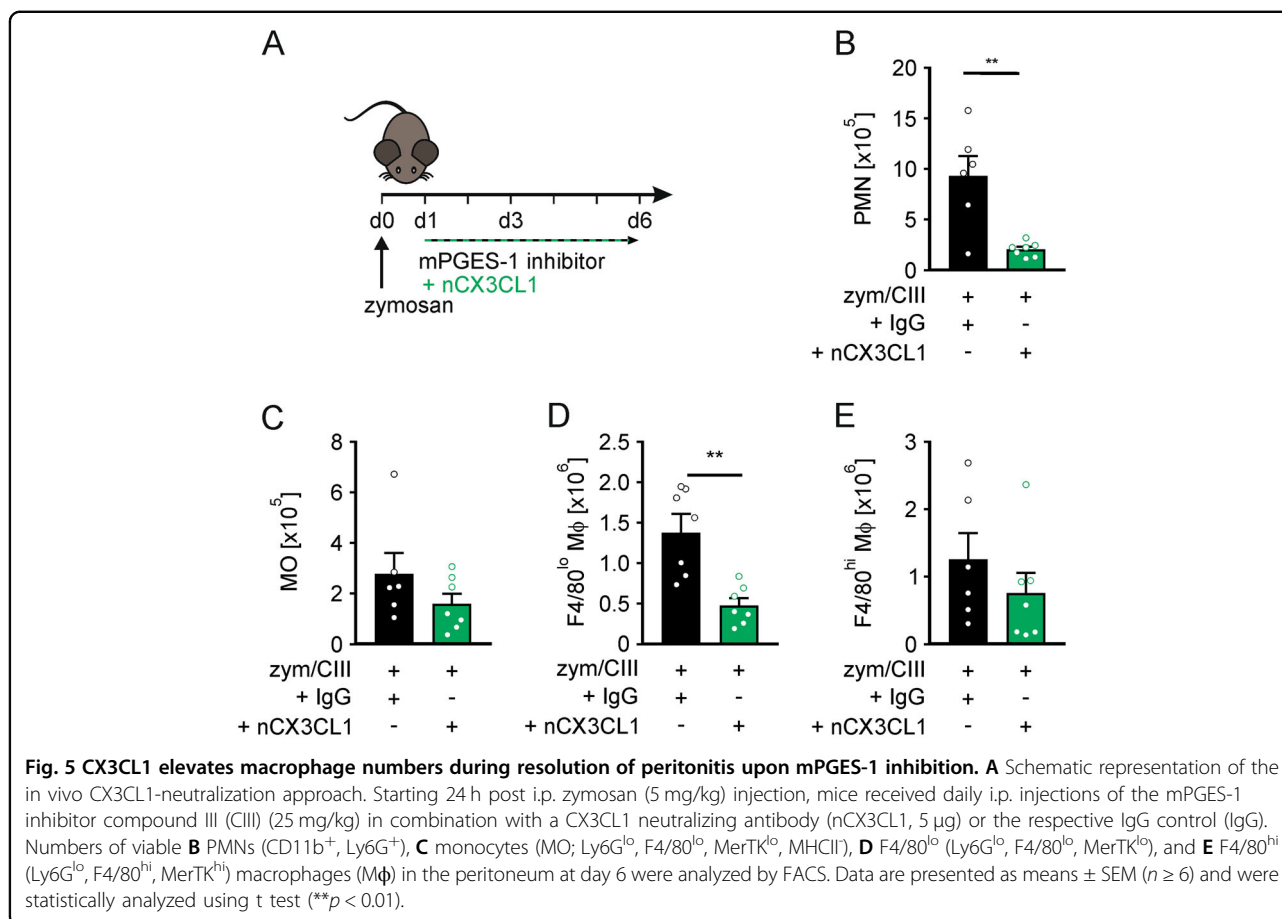
To gain evidence that this concept contributes to the situation in vivo, we administered a neutralizing CX3CL1 antibody (nCX3CL1, 5 µg/day) or the appropriate IgG control (IgG) antibody in combination with the mPGES-1 inhibitor CIII in the peritonitis model (Fig. 5A). Neutralizing CX3CL1 significantly reduced PMN numbers in the peritoneum (Fig. 5B), pointing to normalization of the resolution process. Eliminating CX3CL1 from the system left MO numbers unaltered (Fig. 5C), supporting the

relevance of enhanced adhesion and/or survival of M $\phi$ , rather than MO recruitment. Neutralizing CX3CL1 predominantly reduced the number of F4/80<sup>lo</sup> M $\phi$ , while F4/80<sup>hi</sup> M $\phi$  remained largely unaffected (Fig. 5D, E), despite a marked reduction of CX3CL1 levels (Supplementary Fig. 3).

Conclusively, mPGES-1 contributes to terminate a zymosan-induced peritonitis by limiting epithelial expression of CX3CL1, thereby reconstituting the cellular composition of the peritoneal cavity.

## Discussion

Inflammation is considered a protective mechanism during host defense. To prevent excessive damage of inflamed tissues it is critical to terminate inflammatory processes for efficient recovery<sup>7,36,37</sup>. One of the hallmarks of inflammation and its resolution is the presence and subsequent removal of neutrophils (PMN) at sites of injury. Our finding that the clearance of PMN was attenuated upon mPGES-1 inhibition is in line with a previous report suggesting that PGE<sub>2</sub> promotes the removal of PMN from the site of injury<sup>18</sup>. In this model, PGE<sub>2</sub> induced the production of 12-lipoxygenase (12-LO)-dependent pro-resolving lipid mediators in M $\phi$ , which then contributed to the reverse migration of PMN. While this observation supports the notion that the pro-inflammatory lipid mediator PGE<sub>2</sub> bears resolution properties<sup>15–20</sup>, we did not observe altered expression of 12/15-LO in response to mPGES-1 inhibition, arguing against this axis in our model. Instead, elevated PMN numbers correlated with the increased presence of MO and M $\phi$  during late-stage resolution upon mPGES-1 inhibition, suggesting that the latter rather support PMN infiltration and, thus, hinder the reestablishing of homeostatic conditions. Along the same lines, excess M $\phi$  numbers at sites of inflammation have been shown to favor fibrosis<sup>38,39</sup>, an established outcome of incomplete resolution of acute inflammation. Interestingly, while CX3CR1-expressing M $\phi$  appeared to promote fibrosis, M $\phi$  expressing low levels of CX3CR1 rather contributed to wound healing and tissue repair<sup>27,31,40</sup>. Thus, elevated *Cx3cr1* expression in M $\phi$  late during inflammation upon mPGES-1 inhibition is in line with reports suggesting that PGE<sub>2</sub> contributed to alternative M $\phi$  polarization and wound healing<sup>41</sup>. Accordingly, Cox-2 inhibitors reduced the ability of myofibroblasts to induce alternative activation of M $\phi$ <sup>42</sup>. Since Cox-2 inhibitors attenuate the production of all prostanoids, we feel confident that the use of a mPGES-1 inhibitor allows delineating the role of PGE<sub>2</sub> more specifically. While mPGES-1 inhibitors were reported to redirect the PGE<sub>2</sub> precursor PGH<sub>2</sub> to other prostanoids in vitro<sup>26,43</sup>, we did not observe such shunting in vivo, in line with other reports<sup>44,45</sup>. Epithelial CX3CL1 expression further corroborates previous reports,



demonstrating that CX3CL1 is produced by peritoneal epithelial upon peritoneal dialysis, where it contributed to a fibrotic phenotype<sup>27,46</sup>.

With respect to elevated M $\phi$  numbers upon mPGES-1 inhibition, we observed enhanced adhesion of BMDM in response to CX3CL1, which corroborates previous findings that CX3CL1 increases leukocyte adhesion<sup>47</sup>. Interestingly, *integrin  $\beta$ 7* (*Itgb7*) expression was upregulated in both F4/80<sup>lo</sup> infiltrating and F4/80<sup>hi</sup> resident M $\phi$  during zymosan-induced peritonitis upon mPGES-1 inhibition, and *Itgb7* expression was previously associated with adhesion of B-cells<sup>48</sup> and multiple myeloma cells<sup>49</sup>. Thus, elevated M $\phi$  numbers upon mPGES-1 inhibition might in part be due to enhanced adhesion of M $\phi$  within the peritoneum.

During the course of acute inflammation, F4/80<sup>hi</sup> resident M $\phi$  are usually depleted at the site of injury by emigration and cell death<sup>5,18</sup>. We noticed that inhibition of mPGES-1 effectively prevented depletion of F4/80<sup>hi</sup> M $\phi$ , and, in addition to enhanced *Itgb7* expression, we observed upregulation of anti-apoptotic *Bcl2*, selectively in these cells, which confirms previous reports showing that CX3CL1 enhanced *Bcl2* expression and promoted survival of MO and MO-derived M $\phi$ <sup>34,50</sup>. The observation

that the increase in peritoneal myeloid cells upon mPGES-1 inhibition was reversed upon CX3CL1 neutralization further underscores the crucial role of PGE<sub>2</sub> to limit CX3CL1 signaling for proper resolution of inflammation. While CX3CL1 neutralization completely reversed F4/80<sup>lo</sup>, infiltrating M $\phi$  numbers, F4/80<sup>hi</sup> M $\phi$  were less responsive. Considering that the neutralization approach lowered peritoneal CX3CL1 levels by approximately 50%, these findings may indicate that the CX3CL1-dependent survival increase of F4/80<sup>hi</sup> M $\phi$  is activated at lower CX3CL1 levels, while the adhesion phenotype appears to require higher CX3CL1 concentrations.

In conclusion, we provide evidence that mPGES-1-derived PGE<sub>2</sub> contributes to the resolution of zymosan-induced peritonitis by reducing the expression of epithelial CX3CL1, which allows to reestablishing cellular homeostasis in the peritoneum.

## Material and methods

### Chemicals

All chemicals were purchased from Thermo Fisher Scientific GmbH (Dreieich, Germany), if not indicated otherwise. Primers were ordered from Biomers (Ulm, Germany).

### Peritonitis model

To analyze the course of inflammation *in vivo*, we used the well-established zymosan-induced peritonitis model in mice<sup>51,52</sup>. Specifically, to induce a transient peritonitis, 8–12 week old female C57BL/6 mice received an *i.p.* injection of 5 mg/kg body weight zymosan A (Sigma Aldrich, St. Louis, USA). Starting at day 1 after zymosan injection, mice were randomly selected to receive daily *i.p.* injections of either the mPGES-1 inhibitor compound III (CIII) (25 mg/kg) or the respective vehicle control (1% Tween-80, 0.5% Carboxymethyl cellulose, 0.9% NaCl solution). To neutralize CX3CL1 a CX3CL1 antibody (5 µg/mouse; MAB571, R&D Systems, Minneapolis, USA) was co-injected with CIII. Peritoneal lavages were obtained by flushing the peritoneal cavity with 3 mL phosphate-buffered saline (PBS). Supernatants and cells of the resulting lavages were used for further analyses. Animal experiments followed the guidelines of the Hessian animal care and use committee (approval number: FU/1211).

### FACS sorting

Single-cell suspensions were stained with an antibody mix (Supplementary Table 3) for 20 min at 4 °C in the dark after blocking with FcR blocking reagent (Miltenyi Biotec, Bergisch Gladbach, Germany) in 0.5% bovine serum albumin (BSA) in PBS as previously described<sup>53</sup>. Cells were separated using a FACS ARIA III cell sorter (BD Biosciences, Heidelberg, Germany) to obtain F4/80<sup>lo</sup> and F4/80<sup>hi</sup> Mφ (gating strategy in Supplementary Fig. 1).

### Cells

Bone marrow-derived Mφ (BMDM) were differentiated with 20 ng/mL macrophage colony-stimulating factor (M-CSF), and 20 ng/mL granulocyte-macrophage colony-stimulating factor (GM-CSF) (both Immunotools, Friesoythe, Germany) in Dulbecco's Modified Eagle's Medium (DMEM) (containing 10% fetal calf serum (FCS), 100 U/mL penicillin, 100 µg/mL streptomycin). MO was isolated using the EasySep™ Mouse Monocyte Isolation Kit (Stemcell Technologies, Vancouver, Canada) according to the manufacturer's instructions. E0771 cells were purchased from ATCC-LGC Standards GmbH (Wesel, Germany), maintained in DMEM containing 10% FCS, 100 U/mL penicillin, and 100 µg/mL streptomycin, and routinely tested for mycoplasma.

### Proliferation assay

BMDM were labeled for 20 min with 5 µM carboxy-fluorescein succinimidyl ester (CFSE; Biolegend, San Diego, USA) after 2 days of differentiation. BMDM were then treated with CX3CL1 (100 ng/mL) in the presence of M-CSF or GM-CSF (20 ng/mL each), or exposed to full medium supplemented with lavage fluid isolated at day 6 of the peritonitis experiment at a ratio of 2:1. Cell

numbers and CFSE staining were analyzed 48 h post stimulation by FACS.

### Adhesion assay

BMDM were labeled for 20 min with 5 µM CFSE after 7 days of differentiation. BMDM were then allowed to adhere to fibronectin-coated plates in serum-free DMEM (100 U/mL penicillin, 100 µg/mL streptomycin) for 1 h. Adhesion was measured as cell density by quantifying CFSE intensity using the Spark plate-reader system (Tecan, Männedorf, Switzerland).

### Migration assay

Monocyte (MO) migration was assessed in a Boyden chamber transwell assay (5 µm, Corning, USA). Briefly, MO was added to the upper well of a Boyden chamber in DMEM containing 1% FCS, and allowed to migrate towards CX3CL1 (100 ng/mL) in the lower compartment for 4 h. Migrated cells were stained for CD45, CD11b, and Ly6G and analyzed by FACS.

### RNA sequencing

Total RNA was isolated from sorted F4/80<sup>lo</sup> and F4/80<sup>hi</sup> macrophages (Mφ) using the RNeasy Micro Kit (Qiagen, Hilden, Germany) according to the manufacturer's instructions. RNA concentration and integrity were analyzed with the Qubit HS RNA Assay Kit (Thermo Fisher Scientific) and the Agilent 2100 Bioanalyzer using an RNA 6000 Pico Chip (Agilent Technologies, Waldbronn, Germany), respectively. Sequencing libraries were prepared using the QuantSeq 3' mRNA-Seq Library Prep Kit with the UMI Second Strand Synthesis Module for QuantSeq (Lexogen, Vienna, Austria). Quantity and quality of the cDNA libraries were evaluated by Qubit dsDNA HS Assay Kit (Thermo Fisher Scientific) and Agilent DNA High Sensitivity DNA Chip (Agilent Technologies), respectively. Libraries were sequenced (single end, 75 cycles) using a High Output Kit v2 on a NextSeq 500 sequencer (Illumina, San Diego, USA). Data were analyzed using the Bluebee QuantSeq FWD-UMI Data Analysis Pipeline according to the manual (details see Supplementary Methods). Sequencing data have been deposited under the GEO accession number GSE164364.

### Reverse transcription and quantitative polymerase chain reaction (qPCR)

Total RNA was isolated from sorted cells using the RNeasy Micro kit (Qiagen), followed by amplification and reverse transcription using the MessageBooster kit (Biozym, Hessisch Oldendorf, Germany). qPCR was performed using the PowerUp SYBR Green Mix on Quantstudio PCR Real-Time Systems (Thermo Fisher Scientific) according to the manufacturer's manual (primers in Supplementary Table 4).



### Prostanoid analysis

Prostanoids were quantified as previously described<sup>54</sup> (details are given in Supplementary Methods).

### Immunohistochemistry

Peritoneal membranes from mice at day 6 of the peritonitis model were fixed and paraffin embedded. Deparaffinized and rehydrated membrane sections (4 µm) were stained using the Opal staining system according to the manufacturer's instructions (Perkin Elmer, Waltham, USA) with primary antibodies against CX3CL1 (MAB571, R&D Systems) and pan-cytokeratin (panCK) (ab7753; Abcam, Cambridge, UK). Pictures were acquired with the Vectra Polaris Automated Quantitative Pathology Imaging System featuring MOTiF (Akoya Biosciences, Marlborough, USA). The relative abundance of CX3CL1 expressing cells in the epithelium was scored upon tissue segmentation based on panCK staining with the InForm software (Akoya Biosciences).

### Statistics

Data are presented as means ± SEM of at least three independent experiments. The sample size for each experiment was estimated empirically, according to the exploratory experiments and published literature with similar methodology. Differences were considered significant when \* $p < 0.05$ ; \*\* $p < 0.01$ ; \*\*\* $p < 0.001$ ; ns = not significant. Normal distribution was assessed using D'Agostino–Pearson test. Statistical analysis was done using Student's t test, one-way ANOVA with Holm–Sidak posthoc test (parametric data, otherwise Kruskal–Wallis test), or two-way ANOVA with Holm–Sidak posthoc test (parametric data; otherwise data were log-transformed). Data were statistically evaluated with GraphPad Prism 7.0 (GraphPad Software, USA).

### Acknowledgements

We thank Anica Scholz and Sofia Winslow for critical discussions and Deutsche Forschungsgemeinschaft and the Swedish Research Council for funding.

### Funding

The study was funded by Deutsche Forschungsgemeinschaft (GRK 2336, TP6) and the Swedish Research Council (grant no: 2017-01391). Open Access funding enabled and organized by Projekt DEAL.

### Author details

<sup>1</sup>Institute of Biochemistry I, Faculty of Medicine, Goethe-University Frankfurt, Frankfurt, Germany. <sup>2</sup>Fraunhofer Institute for Translational Medicine and Pharmacology, Frankfurt, Germany. <sup>3</sup>Institute of Clinical Pharmacology, pharmazentrum Frankfurt/ZAFES, University Hospital, Goethe-University Frankfurt, Frankfurt, Germany. <sup>4</sup>Rheumatology Unit, Dep. of Medicine, Solna, Karolinska Institutet, Karolinska University Hospital, Stockholm, Sweden. <sup>5</sup>German Cancer Consortium (DKTK), Partner Site Frankfurt, Frankfurt, Germany. <sup>6</sup>Frankfurt Cancer Institute, Goethe-University Frankfurt, Frankfurt, Germany

### Author contributions

B.B., and T.S. conceived the project; P.R., B.B., and T.S. designed experiments; P.R., S.R., P.M., R.B., A.H., Y.S., D.T., A.W., B.B., and T.S. conducted experiments,

analyzed and interpreted data; G.G., P.-J.J., and B.B. provided technical and material support; P.R., and T.S. wrote the manuscript; P.R., P.-J.J., A.W., B.B., and T.S. edited the manuscript. All authors read and approved the final paper.

### Conflict of interest

The authors declare that they have no conflict of interest.

### Ethics approval

Not applicable.

### Publisher's note

Springer Nature remains neutral with regard to jurisdictional claims in published maps and institutional affiliations.

**Supplementary information** The online version contains supplementary material available at <https://doi.org/10.1038/s41419-021-03423-2>.

Received: 18 November 2020 Revised: 9 January 2021 Accepted: 11 January 2021

Published online: 02 February 2021

### References

- Morgenstern, D. E., Gifford, M. A., Li, L. L., Doerschuk, C. M. & Dinauer, M. C. Absence of respiratory burst in X-linked chronic granulomatous disease mice leads to abnormalities in both host defense and inflammatory response to *Aspergillus fumigatus*. *J. Exp. Med.* **185**, 207–218 (1997).
- Dinauer, M. C. The respiratory burst oxidase and the molecular genetics of chronic granulomatous disease. *Crit. Rev. Clin. Lab. Sci.* **30**, 329–369 (1993).
- Lauber, K., Blumenthal, S. G., Waibel, M. & Wesselborg, S. Clearance of apoptotic cells: getting rid of the corpses. *Mol. Cell* **14**, 277–287 (2004).
- Dalli, J. et al. Annexin 1 mediates the rapid anti-inflammatory effects of neutrophil-derived microparticles. *Blood* **112**, 2512–2519 (2008).
- Gautier, E. L., Ivanov, S., Lesnik, P. & Randolph, G. J. Local apoptosis mediates clearance of macrophages from resolving inflammation in mice. *Blood* **122**, 2714–2722 (2013).
- Fadok, V. A. et al. Macrophages that have ingested apoptotic cells in vitro inhibit proinflammatory cytokine production through autocrine/paracrine mechanisms involving TGF- $\beta$ , PGE<sub>2</sub>, and PAF. *J. Clin. Invest.* **101**, 890–898 (1998).
- Stables, M. J. et al. Transcriptomic analyses of murine resolution-phase macrophages. *Blood* **118**, e192–e208 (2011).
- Dean, R. A. et al. Macrophage-specific metalloelastase (MMP-12) truncates and inactivates ELR+ CXC chemokines and generates CCL2, -7, -8, and -13 antagonists: potential role of the macrophage in terminating polymorphonuclear leukocyte influx. *Blood* **112**, 3455–3464 (2008).
- Lantz, C., Radmanesh, B., Liu, E., Thorp, E. B. & Lin, J. Single-cell RNA sequencing uncovers heterogeneous transcriptional signatures in macrophages during efferocytosis. *Sci. Rep.* **10**, 14333 (2020).
- Watanabe, S., Alexander, M., Misharin, A. V. & Budinger, G. R. S. The role of macrophages in the resolution of inflammation. *J. Clin. Invest.* **129**, 2619–2628 (2019).
- Serhan, C. N. & Savill, J. Resolution of inflammation: the beginning programs the end. *Nat. Immunol.* **6**, 1191–1197 (2005).
- Brown, S. B. & Savill, J. Phagocytosis triggers macrophage release of Fas ligand and induces apoptosis of bystander leukocytes. *J. Immunol.* **162**, 480–485 (1999).
- Newson, J. et al. Resolution of acute inflammation bridges the gap between innate and adaptive immunity. *Blood* **124**, 1748–1764 (2014).
- Kalinski, P. Regulation of immune responses by prostaglandin E<sub>2</sub>. *J. Immunol.* **188**, 21–28 (2012).
- Bystrom, J. et al. Resolution-phase macrophages possess a unique inflammatory phenotype that is controlled by cAMP. *Blood* **112**, 4117–4127 (2008).
- Obermajer, N., Muthuswamy, R., Lesnock, J., Edwards, R. P. & Kalinski, P. Positive feedback between PGE<sub>2</sub> and COX2 redirects the differentiation of human dendritic cells toward stable myeloid-derived suppressor cells. *Blood* **118**, 5498–5505 (2011).

17. Huang, S. K., Wettlaufer, S. H., Chung, J. & Peters-Golden, M. Prostaglandin E2 inhibits specific lung fibroblast functions via selective actions of PKA and Epac-1. *Am. J. Respir. Cell Mol. Biol.* **39**, 482–489 (2008).
18. Loynes, C. A. et al. PGE2 production at sites of tissue injury promotes an anti-inflammatory neutrophil phenotype and determines the outcome of inflammation resolution in vivo. *Sci. Adv.* **4**, eaar8320 (2018).
19. Newson, J. et al. Inflammatory resolution triggers a prolonged phase of immune suppression through COX-1/mPGES-1-derived prostaglandin E2. *Cell Rep.* **20**, 3162–3175 (2017).
20. Tchetina, E. V., Di Battista, J. A., Zukor, D. J., Antoniou, J. & Poole, A. R. Prostaglandin PGE2 at very low concentrations suppresses collagen cleavage in cultured human osteoarthritic articular cartilage: this involves a decrease in expression of proinflammatory genes, collagenases and COL10A1, a gene linked to chondrocyte hypertrophy. *Arthritis Res. Ther.* **9**, R75 (2007).
21. Fuentes, A. V., Pineda, M. D., Venkata & Nagulapalli, KalyanC. Comprehension of top 200 prescribed drugs in the US as a resource for pharmacy teaching, training and practice. *Pharmacy* **6**, 43 (2018).
22. Blobaum, A. L. & Marnett, L. J. Structural and functional basis of cyclooxygenase inhibition. *J. Med. Chem.* **50**, 1425–1441 (2007).
23. Park, J. Y., Pillinger, M. H. & Abramson, S. B. Prostaglandin E2 synthesis and secretion: the role of PGE2 synthases. *Clin. Immunol.* **119**, 229–240 (2006).
24. Hara, S. Prostaglandin terminal synthases as novel therapeutic targets. *Proc. Jpn. Acad. Ser. B Phys. Biol. Sci.* **93**, 703–723 (2017).
25. Bergqvist, F., Morgenstern, R. & Jakobsson, P.-J. A review on mPGES-1 inhibitors: From preclinical studies to clinical applications. *Prostaglandins Other Lipid Mediat.* **147**, 106383 (2020).
26. Lederer, P. et al. Characterization of a human and murine mPGES-1 inhibitor and comparison to mPGES-1 genetic deletion in mouse models of inflammation. *Prostaglandins Other Lipid Mediat.* **107**, 26–34 (2013).
27. Chakarov, S. et al. Two distinct interstitial macrophage populations coexist across tissues in specific subtissular niches. *Science* **363**, eaau0964 (2019).
28. Butenko, S. et al. Transcriptomic analysis of monocyte-derived non-phagocytic macrophages favors a role in limiting tissue repair and fibrosis. *Front. Immunol.* **11**, 405 (2020).
29. Combadiere, C. et al. Identification of CX3CR1. A chemotactic receptor for the human CX3C chemokine fractalkine and a fusion coreceptor for HIV-1. *J. Biol. Chem.* **273**, 23799–23804 (1998).
30. Pan, Y. et al. Neurotactin, a membrane-anchored chemokine upregulated in brain inflammation. *Nature* **387**, 611–617 (1997).
31. Helmke, A. et al. CX3CL1-CX3CR1 interaction mediates macrophage-mesothelial cross talk and promotes peritoneal fibrosis. *Kidney Int.* **95**, 1405–1417 (2019).
32. Imai, T. et al. Identification and molecular characterization of fractalkine receptor CX3CR1, which mediates both leukocyte migration and adhesion. *Cell* **91**, 521–530 (1997).
33. Lucas, A. D. et al. Smooth muscle cells in human atherosclerotic plaques express the fractalkine receptor CX3CR1 and undergo chemotaxis to the CX3C chemokine fractalkine (CX3CL1). *Circulation* **108**, 2498–2504 (2003).
34. Landsman, L. et al. CX3CR1 is required for monocyte homeostasis and atherogenesis by promoting cell survival. *Blood* **113**, 963–972 (2009).
35. Chandrasekar, B. et al. Fractalkine (CX3CL1) stimulated by nuclear factor kappaB (NF-kappaB)-dependent inflammatory signals induces aortic smooth muscle cell proliferation through an autocrine pathway. *Biochem. J.* **373**, 547–558 (2003).
36. Weiss, S. J. Tissue destruction by neutrophils. *N. Engl. J. Med.* **320**, 365–376 (1989).
37. Schett, G. & Neurath, M. F. Resolution of chronic inflammatory disease: universal and tissue-specific concepts. *Nat. Commun.* **9**, 3261 (2018).
38. Wynn, T. A. & Vannella, K. M. Macrophages in tissue repair, regeneration, and fibrosis. *Immunity* **44**, 450–462 (2016).
39. Murray, L. A. et al. TGF-beta driven lung fibrosis is macrophage dependent and blocked by Serum amyloid P. *Int. J. Biochem. Cell Biol.* **43**, 154–162 (2011).
40. Burgess, M., Wicks, K., Gardasevic, M. & Mace, K. A. CX3CR1 expression identifies distinct macrophage populations that contribute differentially to inflammation and repair. *Immunohorizons* **3**, 262–273 (2019).
41. Zhang, S. et al. Prostaglandin E2 hydrogel improves cutaneous wound healing via M2 macrophages polarization. *Theranostics* **8**, 5348–5361 (2018).
42. Fernando, M. R., Giembycz, M. A. & McKay, D. M. Bidirectional crosstalk via IL-6, PGE2 and PGD2 between murine myofibroblasts and alternatively activated macrophages enhances anti-inflammatory phenotype in both cells. *Br. J. Pharm.* **173**, 899–912 (2016).
43. Xu, D. et al. MF63 2-(6-chloro-1H-phenanthro[9,10-dimidazol-2-yl]-isophthalonitrile, a selective microsomal prostaglandin E synthase-1 inhibitor, relieves pyresis and pain in preclinical models of inflammation. *J. Pharm. Exp. Ther.* **326**, 754–763 (2008).
44. Martin, E. M. & Jones, S. L. Inhibition of microsomal prostaglandin E synthase-1 (mPGES-1) selectively suppresses PGE2 in an in vitro equine inflammation model. *Vet. Immunol. Immunopathol.* **192**, 33–40 (2017).
45. Cheng, Y. et al. Cyclooxygenases, microsomal prostaglandin E synthase-1, and cardiovascular function. *J. Clin. Invest.* **116**, 1391–1399 (2006).
46. Ishida, Y. et al. Essential involvement of the CX3CL1-CX3CR1 axis in bleomycin-induced pulmonary fibrosis via regulation of fibrocyte and M2 macrophage migration. *Sci. Rep.* **7**, 16833 (2017).
47. Fong, A. M. et al. Fractalkine and CX3CR1 mediate a novel mechanism of leukocyte capture, firm adhesion, and activation under physiologic flow. *J. Exp. Med.* **188**, 1413–1419 (1998).
48. Gofru, G. et al. Beta7 integrin deficiency suppresses B cell homing and attenuates chronic ileitis in SAMP1/YitFc mice. *J. Immunol.* **185**, 5561–5568 (2010).
49. Neri, P. et al. Integrin beta7-mediated regulation of multiple myeloma cell adhesion, migration, and invasion. *Blood* **117**, 6202–6213 (2011).
50. Karlmark, K. R. et al. The fractalkine receptor CX3CR1 protects against liver fibrosis by controlling differentiation and survival of infiltrating hepatic monocytes. *Hepatology* **52**, 1769–1782 (2010).
51. Doherty, N. S. et al. Intraperitoneal injection of zymosan in mice induces pain, inflammation and the synthesis of peptidoleukotrienes and prostaglandin E2. *Prostaglandins* **30**, 769–789 (1985).
52. Cash, J. L., White, G. E. & Greaves, D. R. in *Chemokines, Part B* (Elsevier, 2009), pp. 379–396.
53. Weichand, B. et al. S1PR1 on tumor-associated macrophages promotes lymphangiogenesis and metastasis via NLRP3/IL-1beta. *J. Exp. Med.* **214**, 2695–2713 (2017).
54. Bärnthaler, T. et al. Imatinib stimulates prostaglandin E2 and attenuates cytokine release via EP4 receptor activation. *J. Allergy Clin. Immunol.* **143**, 794–797.e10 (2019).